High-Efficiency Single-Quantum-Well Green and Yellow-Green Light-Emitting Diodes on Semipolar (20$\bar{2}$1) GaN Substrates

Shuichiro Yamamoto[1,3*], Yuji Zhao[2], Chih-Chien Pan[1], Roy B. Chung[1], Kenji Fujito[4], Junichi Sonoda[1], Steven P. DenBaars[1,2], and Shuji Nakamura[1,2]

[1] *Materials Department, University of California, Santa Barbara, CA 93106, U.S.A.*
[2] *Electrical and Computer Engineering Department, University of California, Santa Barbara, CA 93106, U.S.A.*
[3] *Advanced Technology Research Laboratories, Sharp Corporation, Tenri, Nara 632-8567, Japan*
[4] *Optoelectronics Laboratory, Mitsubishi Chemical Corporation, Ushiku, Ibaraki 300-1295, Japan*

Received September 28, 2010; accepted November 2, 2010; published online November 26, 2010

We demonstrate high-efficiency green and yellow-green single-quantum-well light-emitting diodes (LEDs) grown on semipolar (20$\bar{2}$1) GaN substrates by metal organic chemical vapor deposition. The output power and external quantum efficiency at a driving current of 20 mA under a pulsed condition with a 10% duty cycle are 9.9 mW and 20.4% for the green LED and 5.7 mW and 12.6% for the yellow-green LED, respectively. The electroluminescence linewidth narrowing, which is related to the band-filling effect caused by potential fluctuations, is not observed.

DOI: 10.1143/APEX.3.122102

Wurtzite (Al, Ga, In)N-based semiconductors are attracting much attention as efficient solid-state lighting devices since Nakamura *et al.* commercially achieved high-quality InGaN/GaN multiple-quantum-well (MQW) light-emitting diodes (LEDs) by growing *c*-plane polar GaN on (0001) sapphire substrates.[1)] The performance of commercial blue LEDs grown on *c*-plane sapphire has improved tremendously over the past few years. However, these LEDs grown on *c*-plane sapphire suffer from the quantum confined Stark effect (QCSE) due to the large polarization-related electric fields. This lowers internal quantum efficiency because of the spatial separation of the electron and hole wave functions in the quantum wells (QWs).[2–5)] In addition, the QCSE becomes more significant for longer-wavelength devices such as green LEDs and green laser diodes (LDs) due to the increased lattice mismatch between high-InN-molar-fraction QWs and barriers. As a result, *c*-plane InGaN QWs with high InN molar fraction generally exhibit low quantum efficiency. It is for this reason that the efficiency of green LEDs grown on *c*-plane sapphire has not improved drastically compared with that of blue LEDs. One approach to circumvent these problems is to fabricate LEDs on nonpolar planes such as (11$\bar{2}$0) plane (*a*-plane)[6)] and (10$\bar{1}$0) plane (*m*-plane).[7,8)] However, the output powers of green LEDs on nonpolar planes are still less than 1 mW at a driving current of 20 mA. The other approach is to fabricate LEDs on semipolar planes, which are inclined with respect to the *c*-direction. Several semipolar planes, including (10$\bar{1}\bar{1}$), (11$\bar{2}$2), and other semipolar planes, can be used as growth substrates.[9,10)] In spite of these approaches, the efficiency of green LEDs grown on nonpolar and semipolar planes remains equal to or less than those grown on *c*-plane. The highest external quantum efficiencies (EQEs) of green LEDs ever reported are around 30% on *c*-plane[11)] and 18.9% on (11$\bar{2}$2) plane.[12)] Meanwhile, Enya *et al.* have reported a green LD with a lasing wavelength of 531 nm under a pulsed condition,[13)] and Yoshizumi *et al.* have reported a green LD with lasing wavelength of 520 nm under continuous wave (CW) operation[14)] on novel semipolar (20$\bar{2}$1) GaN substrates. Further studies have shown that green emitting QWs grown on (20$\bar{2}$1) plane exhibit high compositional homogeneity with localization energy values lower than those reported for *c*-plane.[15)] However, only few reports on characterizations of green LEDs grown on (20$\bar{2}$1) plane have been published.[16)] In this paper, we demonstrate the growth and fabrication of high-efficiency green and yellow-green LEDs on (20$\bar{2}$1) semipolar GaN substrates.

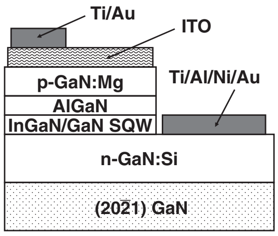

Fig. 1. A schematic figure of the green and yellow-green LED device structures on (20$\bar{2}$1) substrate.

The semipolar GaN LEDs were grown on (20$\bar{2}$1) GaN substrates by metal organic chemical vapor deposition (MOCVD). The (20$\bar{2}$1) substrates were sliced from *c*-plane GaN bulk crystals grown by hydride vapor phase epitaxy (HVPE) at Mitsubishi Chemical. The LED structures consisted of 1 μm Si-doped n-GaN, followed by an active region, which consisted of a 3.5 nm-thick InGaN single quantum well (SQW) and GaN barriers. The typical growth temperature of the active region is 780 °C for the green LED and 760 °C for the yellow-green LED. A 20-nm-thick Mg-doped p-AlGaN electron blocking layer was grown after the active region, followed by a p-GaN layer and p^+-GaN contact layer. Lateral LEDs with 490 × 292 μm^2 mesa size were fabricated by conventional photolithography. A 250 nm-thick SnO_2-doped In_2O_3 (ITO) layer was deposited by electron beam deposition and annealed by rapid thermal annealing (RTA) as the p-type transparent contact. The n-contact, consisting of a Ti/Al/Ni/Au (10/100/10/100 nm) metal stack, was deposited on n-GaN, and then a Ti/Au (20/300 nm) metal stack was deposited as a pad electrode on ITO. A schematic figure of the device structure is shown in Fig. 1. To improve light extraction efficiency, we introduced a backside roughening technique.[17)] Wafers were diced, and then individual LEDs were mounted on a transparent ZnO vertical stand as a submount and packaged with silicone resin.[18)]

*E-mail address: yamamoto.shuhichiroh@sharp.co.jp

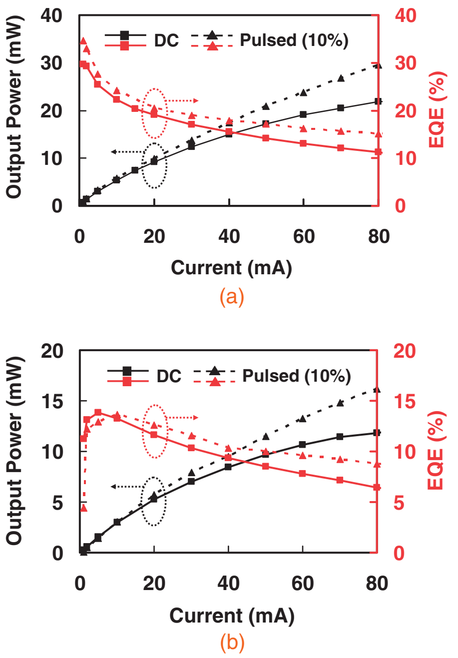

Fig. 2. The output power and external quantum efficiency of (a) green LED and (b) yellow-green LED as a function of driving current under DC condition and pulsed condition with 10% duty cycle.

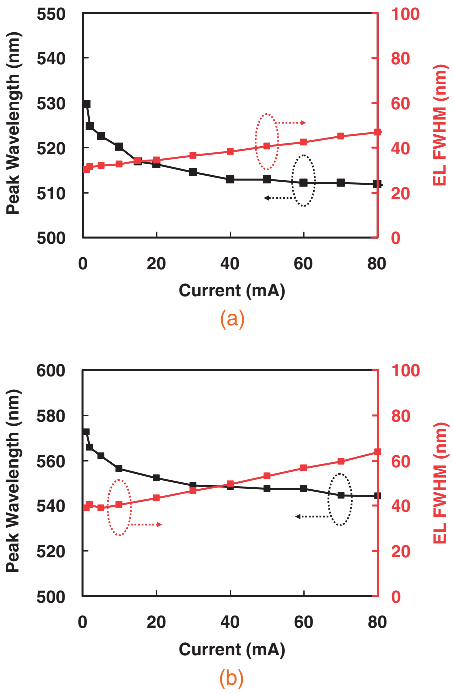

Fig. 3. The EL peak wavelength and FWHM of (a) green LED and (b) yellow-green LED as a function of driving current under DC condition.

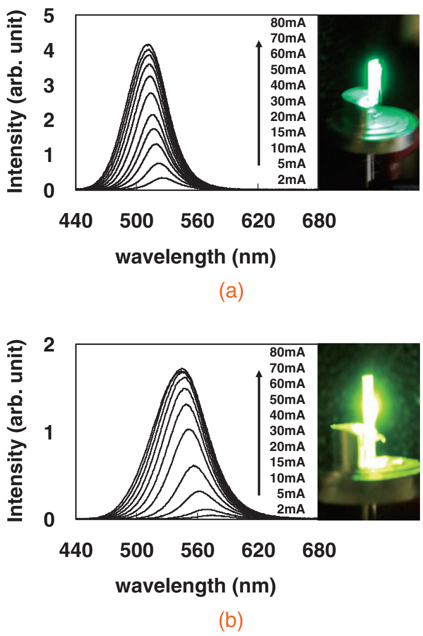

Fig. 4. Dependence of the electroluminescence spectra on driving current under DC condition and optical micrograph of (a) green LED and (b) yellow-green LED at a driving current of 10 mA.

Electroluminescence (EL) measurements were carried out at room temperature (RT) under a direct current (DC) condition and a pulsed condition with a 10% duty cycle. We illustrate the data under the DC condition unless otherwise stated. The packaged LEDs were tested by a calibrated integrating sphere.

The dependences of output power and EQE with increasing driving current are shown in Figs. 2(a) and 2(b) for the green and yellow-green LEDs, respectively. EL spectra with increasing current are shown in Figs. 3(a) and 3(b). The dependence of peak wavelength and the full width at the half maximum (FWHM) with increasing current are shown in Figs. 4(a) and 4(b). Also, the current–voltage (I–V) characteristics are shown in Fig. 5.

For the green LED, at a driving current of 20 mA, the output power and EQE are 9.9 mW and 20.4% under the pulsed condition and 9.2 mW and 19.1% under the DC condition, respectively. The peak wavelengths are 529.9, 516.3, and 511.9 nm at currents of 1, 20, and 80 mA, respectively. The wavelength shift with increasing injection current from 1 to 20 mA is 13.6 nm. This amount of blue shift is comparable to that of a green LED grown on $(11\bar{2}2)$ plane[12)] and a commercial LED on c-plane.[9)] We speculated this observed blue shift at a low-current is due to both the band-filling effect caused by potential fluctuations and the QCSE. However, only the broadening of the emission linewidth is observed regardless of the size of the injection current. This is an important difference from green LEDs grown on $(11\bar{2}2)$ plane, in which marked narrowing of the emission linewidth is observed in the low-current range.[12,19)] This result indicates that the band-filling effect contributes to only a little part of the blue shift in the green LED on the $(20\bar{2}1)$ plane because the band-filling effect induces the blue shift accompanied by narrowing in the low-current range.[19)] We assume that the localized states having lower energy induced by potential fluctuations are saturated with increasing current, which leads to an additional blue shift and the emission linewidth narrowing. Therefore, the absence of the narrowing in the green LED on $(20\bar{2}1)$ plane indicates that the band-filling effect is limited in the low-current range. For this reason, we deduced that the uniformity of the InGaN QW is substantially improved by growing LEDs on $(20\bar{2}1)$ plane. However, further study is needed to clarify the more detailed relationship between the blue shift and the emission linewidth narrowing, including the comparison with that

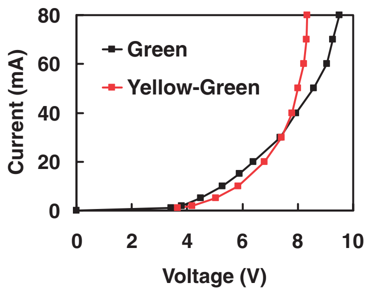

Fig. 5. Current–voltage (*I*–*V*) characteristics of green LED and yellow-green LED.

relationship in the green LED on *c*-plane, which is infrequently-reported ever.[20)]

The wavelength shift with increasing current from 20 to 80 mA is 4.4 nm in the green LEDs on $(20\bar{2}1)$ plane. This blue shift is much smaller than that of the green LED on $(11\bar{2}2)$ plane, which is 12.4 nm with increasing current from 20 to 100 mA.[21)] In addition to screening of the polarization-induced electric field by carrier injection, since the band-filling effect is also the primary origin of the blue shift in this current range, the smaller blue shift indicates presence of fewer potential fluctuations. However, since the net blue shift measured under the DC condition is the value compensated by the red shift caused by the self-heating, further detailed investigation, in which the self-heating effect is taken into account, is required in this high-current range.

For the yellow-green LED, at a driving current of 20 mA, the output power and EQE are 5.7 mW and 12.6% under the pulsed condition and 5.2 mW and 11.6% under the DC condition, respectively. The peak wavelengths are 572.5, 552.3, and 544.2 nm at currents of 1, 20, and 80 mA, respectively. Identically to the green LED, a large blue shift is observed at a low current. The wavelength shift with increasing injection current from 20 to 80 mA is 8.1 nm, which is larger than that of the green LED on $(20\bar{2}1)$ plane. This indicates that the high In composition of the yellow-green LED leads to more significant potential fluctuations than those in the green LED. However, the blue shift with increasing injection current from 20 to 80 mA is still smaller than that of the green LED on $(11\bar{2}2)$ plane. Additionally, the emission linewidth narrowing is not observed. This indicates that the band-filling effect is limited in the low-current range as mentioned above. These results indicate that $(20\bar{2}1)$ plane is suitable for growing LEDs with not only green wavelengths but also even longer wavelengths. This is also confirmed by comparing the emission linewidths. The emission linewidths with a driving current of 10 mA are 33.0 and 40.8 nm for the green and yellow-green LEDs on $(20\bar{2}1)$ plane, respectively, and 42.5 nm for the green LEDs on $(11\bar{2}2)$ plane.[21)] The narrower linewidth indicates presence of fewer potential fluctuations.

The operating voltages at a driving current of 20 mA are 6.4 and 6.8 V for the green and yellow-green LEDs, respectively. We attribute the high operation voltages to the unoptimized growth conditions of the p-GaN layers and the ITO contact electrodes.

In summary, SQW green and yellow-green LEDs were fabricated on semipolar $(20\bar{2}1)$ GaN substrates. For the green LED, the output power and EQE at a driving current of 20 mA are 9.9 mW and 20.4% under the pulsed condition and 9.2 mW and 19.1% under the DC condition, respectively. To the best of our knowledge, these output powers and EQEs at a driving current of 20 mA are the highest values that have ever been reported for green LEDs grown on semipolar/nonpolar planes. For the yellow-green LED, the output power and EQE at a current of 20 mA are 5.7 mW and 12.6% under the pulsed condition and 5.2 mW and 11.6% under the DC condition, respectively. The EL linewidth narrowing, which is related to the band-filling effect caused by potential fluctuations, is not observed in the low-current range. This indicates that the uniformity of the InGaN QW is substantially improved by growing LEDs on $(20\bar{2}1)$ plane. These results suggest that $(20\bar{2}1)$ GaN substrates could be one of the possible substrates for high-power and high-efficiency LEDs with green or even longer wavelengths.

Acknowledgments The authors acknowledge the Solid State Lighting and Energy Center at UCSB for funding. A portion of this work was done in the UCSB nanofabrication facility, part of the National Science Foundation (NSF) funded National Nanotechnology Infrastructure Network (NNIN) network. This work made use of the Central Facilities at UCSB supported by the NSF Materials Research Science and Engineering Centers (MRSEC).

1) S. Nakamura, T. Mukai, M. Senoh, S. Nagahama, and N. Iwasa: J. Appl. Phys. **74** (1993) 3911.
2) S. Chichibu, T. Azuhata, T. Sota, and S. Nakamura: Appl. Phys. Lett. **69** (1996) 4188.
3) A. Hangleiter, J. S. Im, H. Kolmer, S. Heppel, J. Off, and F. Scholz: MRS Internet J. Nitride Semicond. Res. **3** (1998) 15.
4) F. Bernardini and V. Fiorentini: Phys. Status Solidi B **216** (1999) 391.
5) A. E. Romanov, T. J. Baker, S. Nakamura, and J. S. Speck: J. Appl. Phys. **100** (2006) 023522.
6) T. Detchprohm, M. Zhu, Y. Li, Y. Xia, C. Wetzel, E. A. Preble, L. Liu, T. Paskova, and D. Hanser: Appl. Phys. Lett. **92** (2008) 241109.
7) K. Okamoto, H. Ohta, D. Nakagawa, M. Sonobe, J. Ichihara, and H. Takasu: Jpn. J. Appl. Phys. **45** (2006) L1197.
8) Y. Lin, A. Chakraborty, S. Brinkley, H. C. Kuo, T. Melo, K. Fujito, J. S. Speck, S. P. DenBaars, and S. Nakamura: Appl. Phys. Lett. **94** (2009) 261108.
9) R. Sharma, P. M. Pattison, H. Masui, R. M. Farrel, T. J. Baker, B. A. Haskell, F. Wu, S. P. DenBaars, J. S. Speck, and S. Nakamura: Appl. Phys. Lett. **87** (2005) 231110.
10) H. Masui, T. J. Baker, M. Iza, H. Zhong, S. Nakamura, and S. P. DenBaars: J. Appl. Phys. **100** (2006) 113109.
11) P. Stauss, A. Walter, J. Baur, and B. Hahn: presented at 7th Int. Conf. Nitride Semiconductors (ICNS7), 2007.
12) H. Sato, H. Hirasawa, H. Asamizu, N. Fellows, A. Tyagi, M. Saito, K. Fujito, J. S. Speck, S. P. DenBaars, and S. Nakamura: J. Light Visual Environ. **32** (2008) 107.
13) Y. Enya, Y. Yoshizumi, T. Kyono, K. Akita, M. Ueno, M. Adachi, T. Sumitomo, S. Tokuyama, T. Ikegami, K. Katayama, and T. Nakamura: Appl. Phys. Express **2** (2009) 082101.
14) Y. Yoshizumi, M. Adachi, Y. Enya, T. Kyono, S. Tokuyama, T. Sumitomo, K. Akita, T. Ikegami, M. Ueno, K. Katayama, and T. Nakamura: Appl. Phys. Express **2** (2009) 092101.
15) M. Funato, A. Kaneta, Y. Kawakami, Y. Enya, K. Nishizuka, M. Ueno, and T. Nakamura: Appl. Phys. Express **3** (2010) 021002.
16) R. B. Chung, Y. Lin, I. Koslow, N. Pfaff, H. Ohta, J. Ha, S. P. DenBaars, and S. Nakamura: Jpn. J. Appl. Phys. **49** (2010) 070203.
17) Y. Zhao, J. Sonoda, C. C. Pan, S. Brinkley, I. Koslow, K. Fujito, H. Ohta, S. P. DenBaars, and S. Nakamura: Appl. Phys. Express **3** (2010) 102101.
18) C. Pan, I. Koslow, J. Sonoda, H. Ohta, J. Ha, S. Nakamura, and S. P. DenBaars: Jpn. J. Appl. Phys. **49** (2010) 080210.
19) M. Funato, M. Ueda, Y. Kawakami, Y. Narukawa, T. Kosugi, M. Takahashi, and T. Mukai: Jpn. J. Appl. Phys. **45** (2006) 659.
20) P. D. Mierry, T. Guehne, M. Nemoz, S. Chenot, E. Beraudo, and G. Nataf: Jpn. J. Appl. Phys. **48** (2009) 031002.
21) H. Sato, A. Tyagi, H. Zhong, N. Fellows, R. B. Chung, M. Saito, K. Fujito, J. S. Speck, S. P. DenBaars, and S. Nakamura: Phys. Status Solidi: Rapid Res. Lett. **1** (2007) 162.